

Cite this: DOI: 10.1039/c0xx00000x

www.rsc.org/xxxxxx

Temperature & pH triggered release characteristics of water/fluorescein from 1-ethyl-3-methylimidazolium ethylsulfate based ionogels.

Simon Gallagher^a, Andrew Kavanagh^a, Larisa Florea^a, Douglas R. MacFarlane^b, Kevin J. Fraser^a and Dermot Diamond^{*a}.

⁵ Received (in XXX, XXX) Xth XXXXXXXXXX 20XX, Accepted Xth XXXXXXXXXX 20XX

DOI: 10.1039/b000000x

A crosslinked Poly(*N*-isopropylacrylamide) ionogel encapsulating an ionic liquid exhibits improved transmittance properties, enhanced water uptake/release, greater thermal actuation behaviour and distinct solvatomorphology over its hydrogel equivalent. It was also found that the rate of release of fluorescein pre-loaded into membranes was considerably enhanced for ionogels compared to equivalent hydrogels, and could be triggered through changes in pH and temperature.

Poly(*N*-isopropylacrylamide) (pNIPAAm) hydrogels have been the subject of particular attention due to their well-known actuation behaviour¹. This expansion/contraction behaviour is associated with a temperature threshold, known as the Lower Critical Solution Temperature (LCST)². pNIPAAm based hydrogels have been shown to swell and solvate important pharmacological substances, and subsequently release these substances as the polymer contracts above its LCST³. It has been demonstrated previously that the pNIPAAm LCST threshold can be fine tuned depending on the polymer composition⁴. This requires chemical modification of the polymer backbone and, as a general rule, hydrophilic modifications have been shown to lower the LCST⁵. However, the brittleness and inflexibility of pNIPAAm at high crosslink densities in the dehydrated state can pose handling problems⁶. Even more importantly, water volatility means the lifetime of pNIPAAm-based hydrogels is dramatically reduced when used in open atmospheres⁷.

A novel alternative proposed by some has been to replace the aqueous phase of these materials with Ionic Liquids (ILs)⁸. The employment of ILs as a replacement for water in gel-based polymers has led to the emergence of ionogels as a relatively new sub-class of materials. To date, ionogels have been the subject of reviews detailing their preparation, and their applications in sensor science⁹. The ionogel template is an ideal matrix as the properties of the IL are hybridised with those of the polymer component combining the favourable characteristics of both independent phases in one material.

As pNIPAAm is well known as a platform for drug delivery, dyes have been used such as Methylene blue¹⁰ and Orange II¹¹ to monitor their uptake and release properties of the hydrogels. The study of release of pre-loaded organic molecules is of great interest for example as a model platform for precise delivery

(space, time, amount) of active drugs (in vitro). In order to study the effect of temperature and pH on the release characteristics of organic molecules (Fig S1) loaded into ionogels, we used fluorescein as a model compound due to its ease of optical visualization¹². It is well known that Fluorescein can exist in several isomeric forms dependent on the pH (Fig S2). It is also an excellent probe due to its high quantum yield, absorption (λ_{max} 494 nm) and emission (λ_{max} 521 nm) in the visible region of the spectrum¹².

In this work, rheometry was used to quantify the change in mechanical moduli of two polymer gel templates (hydrogel vs a 1-ethyl-3-methylimidazolium ethylsulfate ([C₂mIm][EtSO₄]) based ionogel) as a function of temperature, and scanning electron microscopy was employed to investigate differences in the solvatomorphological microstructures. Gel samples were loaded with fluorescein (3 mM) and exposed to water buffered at pH 4.0, 7.0 and 9.2, with the dynamics of fluorescein release observed using video imaging and by measuring the concentration of fluorescein in the bathing solution after 1 min. The experiments were repeated using the same buffers for water above and below the LCSTs of the gels (40 °C and 20 °C, respectively).

It was found that the two gels display differences in physical characteristics after polymerisation. For example, it is evident that the ionogel is more flexible and transparent than the equivalent hydrogel (Figure S3 (a, b)). Unlike ILs, which have negligible vapour pressure under ambient conditions, water is gradually lost from the hydrogels and the material becomes increasingly brittle over time. Additionally, the rate constant obtained for the rate of water uptake for the ionogel was found to be ~ 30 times larger (Figures S4 and S5).

The neat hydrophilic IL undergoes a 96.3 % change in viscosity under ambient conditions, when mixed with water in a 1:1 v/v ratio (Table S1 Fig S6). As the ionogel is essentially anhydrous at the outset, the chemical potential drive for water absorption into the hydrophilic IL is large. As a result, ionogel structures swell considerably on exposure to water. For example, the diameter of ionogel disks increased by 30% above their initial value, in some of the structures we have worked with (Table 1 & Table S2). Similar to chemical modifications of the polymeric backbone, the ionogel LCST can be considerably affected by the presence of the IL (Table 1, Figure S7).

Above the LCST the ionogel contracts by 31.4 % of its initial swollen diameter indicating expulsion of the absorbed water and some of the IL originally present, whereas the equivalent hydrogel was found to swell by 18.6% and contract by 21.6%.

Sample	LCST ($^{\circ}\text{C}$)	Dehydrated gel diameter (mm)	(a) Swelling % increase	(b) Contraction % decrease
Ionogel	26	3.46	28.7	31.4
Hydrogel	31	3.25	18.6	21.6

Table 1: Increase in disc diameter from dehydrated state to (a) fully hydrated state at $T = 20^{\circ}\text{C}$ ($n = 3$). (b): Decrease in disc diameter from fully hydrated state (a) when $T = 40^{\circ}\text{C}$ ($n = 3$).

The difference in actuation % between the hydrogel and ionogel can be attributed to the presence of the IL within the polymer network. It is well known that lower cross linking density results in increased water uptake, however this can result in a weaker mechanical stable gel. Therefore a compromise between physical/mechanical integrity (high degree of cross linking) and extent of actuation (low degree of cross-linking) has been established for these materials.

For viscoelastic materials, rheology experiments (Figure 1 & S8) provide information about the storage modulus (energy stored in the material) and the loss modulus (energy dissipated as heat) of these gels. These parameters are commonly used to characterise general mechanical properties of such materials. The rheology experiments were designed to enable the behaviour of the sample to be monitored in both its swollen and contracted states over a period of 15 min.

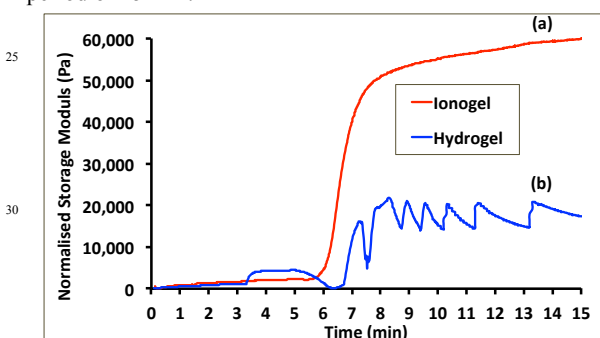


Figure 1: Storage moduli as a function of LCST phase transition for (a) Ionogel and (b) hydrogel (Heating Rate: 20°C to 45°C at 20°C per min starting after 5 minutes).

Initially (0 to 5 min), both gels are in their hydrated states below the LCST (20°C), and the shear rate frequency is kept constant. It can clearly be seen from Figure 1 that the ionogel exhibits a stable mechanical response over this time period. Under the same experimental conditions the brittle hydrogel's mechanical stability is sporadic and fluctuates across a $\sim 3,000$ Pa range. At $t = 5$ min, the sample plate is heated from 20 to 45°C , ensuring that any thermally sensitive processes related to the LCST are completed in both samples. As the temperature is increased, the storage modulus increases in tandem as the polymer contracts and its mechanical energy is stored internally in response to the applied stress. The increase in the storage modulus of the hydrogel is erratic at higher temperatures. This reflects the materials inability to maintain the stored energy as it contracts, indicative of a material with fragile mechanical stability¹³. The more consistent ionogel thermo-responsive

behaviour is evident as the temperature is increased, with the substantially increased storage modulus plateauing at approximately 10 minutes. Thus it yields a much more energetically stable contracted gel compared to the hydrogel under these conditions.

The corresponding loss moduli of both gel platforms were found to correlate with the temperature dependent storage moduli features (Fig S8). From the point of view of the liquid phase therefore, the ionogel displays an increased dissipation of the converted energy over the hydrogel control. Thus, from the rheological effects described, the ionogel displays improved viscoelastic properties compared to the hydrogel. Significantly, this means that a relatively high density of cross-linking sites can exist within a yet flexible ionogel material.

An interesting feature of pNIPAAm is its contrasting porosities as the preparation solvent is varied. Solvatomorphological affects have been found to correlate with the mole fraction of the formulation solvent¹⁴, and with the use of porosogens, such as biologically prevalent sugars¹⁵. Figure S9 shows the effect of hydration on the hydrogel surface morphology, changing from a relatively dense ribbed type surface (a) to a much more swollen form (b). Under equivalent conditions, the ionogel has a distinctly different surface morphology in the non-hydrated and hydrated states (Figure S10 (a) and (b), respectively). In its initial non-hydrated state, the ionogel displays a highly porous, nodule type morphology, efficiently pre-disposed for water uptake. As the hydration process proceeds, the morphology changes, clearly evolving to a more swollen state.

Due to the ionogel's very effective hydration characteristics, and its relatively low LCST, we investigated its possible use for the thermally controlled release of solvated organic molecules, using fluorescein as a model system. Table 2 & Table S3 express the quantity of fluorescein expelled after one minute above/below the LCST under acidic, neutral and basic conditions, for the hydrogel and the ionogel. The results show that at over the pH range 4.0 - 9.2, when the temperature is below the LCST ($T = 20^{\circ}\text{C}$), the release of fluorescein is minimal for both gels (Table 2 and Figure S11). However, at pH 4, and 40°C (i.e; $T > \text{LCST}$ for both gels), there is a striking difference in the rate at which fluorescein is released from the ionogel. Samples taken from the ionogel bathing solution after 1 minute show a fluorescein concentration of 0.3 mM, compared to negligible concentrations in the hydrogel bathing solution. When the temperature is held above the LCSTs ($T = 40^{\circ}\text{C}$), the rate of release of fluorescein increases for both gels with increasing pH, but the rate of release is always greater for the ionogel.

There are several interesting outcomes arising from these experiments. For both gels, fluorescein release is clearly dependent on whether the temperature is above or below the LCST. As the capacity for polymer-fluorescein interactions decrease (due to increasing polymer-polymer interactions), the fluorescein-solvent interactions increase, manifesting in an increase in the rate of fluorescein release ($T > \text{LCST}$). This effect is further enhanced in the ionogel due to stronger interactions between the solvent (H-bonding, electrostatic interactions) and fluorescein. In general, fluorescein release is favoured when $T > \text{LCST}$ and release is impaired when $T < \text{LCST}$. For both gels, fluorescein release is enhanced as the pH is increased (pH 9.2 >

pH 7.0 > pH 4.0) and finally the fluorescein release is enhanced by the presence of the $[C_2mIm][EtSO_4]$ in the gel (ionogel > hydrogel). These trends can be explained as follows; when the gels are above the LCST, solvent (IL, water) and solute (fluorescein) interactions with the polymer backbone (e.g. hydrogen bonding with pNIPAAm amide groups) are reduced in favour of increasingly strong polymer-polymer hydrogen bonding as the gel contracts, adopting a more compact format, which also reduces the free volume available for the solvent/solute to occupy. This effect is more apparent in the ionogel than the hydrogel, leading to a 31.4% dimension change in the diameter of ionogel discs compared to 21.5% for equivalent hydrogel disks.

	Hydrogel (mM)		Ionogel (mM)	
	< LCST	> LCST	< LCST	> LCST
pH 4	-	-	-	0.3023 (2.96×10^{-4})
pH 7	-	0.0082 (4.97×10^{-5})	-	0.3510 (1.57×10^{-2})
pH 9.2	-	0.1970 (1.20×10^{-3})	-	0.5382 (4.49×10^{-2})

Table 2: Concentration of fluorescein (mM) found in the bathing solution for both gels below the LCST (20 °C,) and above the LCST (40 °C) after 1 min. Standard deviation is presented in brackets (n = 3).

Therefore, the rate of release of the loaded fluorescein is enhanced above the LCST for both gels, and the effect is greater for the ionogel than the hydrogel.

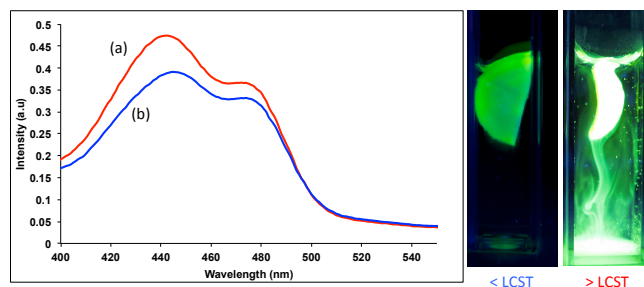


Figure 2: Left: Absorbance spectra obtained for the Fluorescein dye in (a) pH 4 buffered solution and (b) 1:1 (v/v) pH 4 buffered/ $[C_2mIm][EtSO_4]$ solution after 1 min. Right: Snapshot images of the ionogel after 30 seconds in pH 4 buffered solution above and below its LCST.

The general increase in rate of release of fluorescein with increasing pH is related to the deprotonation of fluorescein from the neutral quinoid form (hydrogen bonding interactions favoured) to the monoanion and dianion forms (Fig S2). The increasing charge on fluorescein renders it more soluble in water and hence more mobile (rate of release generally increases). The presence of the IL enhances the effectiveness of electrostatic interactions with the anionic forms of fluorescein that predominate at pH 7 and pH 9.2 (Figure S12, S13), and therefore solvation (and release) is enhanced compared to the equivalent hydrogel ($T > LCST$). Confirmed trace amounts of IL in the released solution above the LCST was detected by Raman spectroscopy (Figure S18).

The dramatic enhancement in release of fluorescein at pH 4 observed with the ionogel compared to the hydrogel most likely arises as, at this pH, fluorescein tends to exist predominantly in the neutral (quinoid) form, as shown by the absorbance spectra in figure 2. In the presence of $[C_2mIm][EtSO_4]$, the absorbance

bands are reduced, suggesting that the neutral quinoid form is, to some extent, converted to the non-absorbing zwitterionic neutral form due to the presence of sp^3 hybridization which disrupts the conjugation of π -blonds in the xanthene moiety of the fluorescein¹⁶. The zwitterionic isomer will tend to be stabilized by electrostatic interactions with the IL, rendering it more mobile than the quinoid form, in which hydrogen bonding is the dominant inter-molecular force. Therefore for the hydrogel (pH4, $T > LCST$), we observe negligible amounts of fluorescein in the bathing solution after 1 minute. Whereas, for the ionogel, a strong flux can be clearly seen in the video under the same conditions, and a significant concentration of fluorescein is found in the bathing solution after 1 minute (0.30 mM, table 2). These results suggest that for these gels, the release of a loaded molecule can be turned on/off by bringing the temperature above/below the LCST, respectively. In addition, the rate of release of pre-loaded molecules can be tuned by controlling the %v/v of IL in the gel formulation, and by changing the pH.

Notes and references

We acknowledge support under the Marie Curie IRSES-MASK project (PIRSES-GA-2010-269302), Science Foundation Ireland grant 07/CE/I1147), Marie Curie Actions re-integration grant PIRG07-GA-2010-268365 (for K.J.F) and the Irish Research Council. D.R.M. is grateful to the Australian Research Council for a Federation fellowship.

^a CLARITY, The Centre for Sensor Web Technologies, National Centre for Sensor Research, School of Chemical Sciences, Dublin City University, Dublin, Ireland. Tel: +353 1 700 5404; E-mail:

^b Dermot.diamond@dcu.ie

^c School of Chemistry, Monash University, Wellington Road, Clayton, 3800, Australia.

† Electronic Supplementary Information (ESI) available: Gel fabrication, IL/water physicochemical data, SEM imaging, Fluorescence Spectroscopy, DSC thermal plots and fluorescein expulsion rate videos. See DOI: 10.1039/b000000x/

1. F. Benito-Lopez, R. Byrne, A. M. Raduta, N. Vrana, G. McGuinness and D. Diamond, *Lab on a chip*, 2010, **10**, 195-396.
2. H. G. Schild, *Progress in Polymer Science*, 1992, **17**, 163-249.
3. A. Chilkoti, M. R. Dreher, D. E. Meyer and D. Raucher, *Advanced Drug Delivery Reviews*, 2002, **54**, 613-630.
4. H. Ringsdorf, J. Venzmer and F. M. Winnik, *Macromolecules*, 1991, **24**, 1678-1686.
5. U. Rauwald, J. del Barrio, X. J. Loh and O. A. Scherman, *Chem. Comm*, 2011, **47**, 6000-6002.
6. T. Friedrich, B. Tieke, F. J. Stadler and C. Bailly, *Soft Matter*, 2011, **7**, 6590-6597.
7. J. Hoffmann, M. Plotner, D. Kuckling and W. J. Fischer, *Sensors and Actuat A-Physical*, 1999, **77**, 139-144.
8. T. Ueki and M. Watanabe, *Macromolecules*, 2008, **41**, 3739-3749.
9. A. Kavanagh, R. Byrne, D. Diamond and K. J. Fraser, *Membranes*, 2012, **2**, 16-39.
10. B. Taşdelen, N. Kayaman-Apohan, O. Güven and B. M. Baysal, *Polym. Adv. Technol.*, 2004, **15**, 528-532.
11. M. R. Guilherme, E. A. Toledo, A. F. Rubira and E. C. Muniz, *J. Memb. Sci*, 2002, **210**, 129-136.
12. M. M. Martin and L. Lindqvist, *J. Lumin.*, 1975, **10**, 381-390.
13. P. Hiemenz and T. P. Lodge, *Polymer Chemistry*, Florida, 2007.
14. C. S. Biswas, V. K. Patel, N. K. Vishwakarma, A. K. Mishra, R. Bhimireddi, R. Rai and B. Ray, *J. App. Pol. Sci*, 2012, **125**, 2000-2009.
15. X.-Z. Zhang, X.-D. Xu, S.-X. Cheng and R.-X. Zhuo, *Soft Matter*, 2008, **4**, 385-391.
16. M. Ali, P. Dutta and S. Pandey, *J. Phys. Chem. B*, 2010, **114**, 15042-15051.